Tomographic imaging of molecular orbital with high harmonic generation

Itatani, J.; Levesque, J.; Zeidler, D.; Spanner, M.; Corkum, P. B.; Villeneuve, D. M.

National Research Council Canada   Conseil national de recherches Canada

Canada

Tomographic Imaging of Molecular Orbitals with High-Harmonic Generation

J. Itatani[1, 2], J. Levesque[1, 3], D. Zeidler[1], H. Niikura[1], P. B. Corkum[1], and D. M. Villeneuve[1, *]

[1] *National Research Council of Canada, 100 Sussex Drive, Ottawa, Ontario K1A 0R6, Canada*
[2] *University of Ottawa, 150 Louis Pasteur, Ottawa, Ontario K1N 6N5, Canada*
[3] *INRS-Energie et Materiaux, Varennes, Québec J3X 1S2, Canada*
*e-mail: david.villeneuve@nrc.ca
Received September 29, 2004

Abstract—High harmonics produced in aligned molecules contain structural information on bound electronic states. We have produced high harmonics from N_2 molecules aligned in five directions relative to the laser polarization axis. The projected images of the highest molecular orbital (HOMO) are successfully reconstructed based on computed tomography using the observed harmonic spectra. The reconstructed wavefunction includes both amplitude and phase. We also show that attosecond bound-state electron wavepacket dynamics will manifest itself in the high-harmonic spectra.

Although the total electron density in molecules is routinely measured by X-ray diffraction or electron scattering, only two methods are able to "see" the highest occupied molecular orbitals (HOMO)—electron-momentum spectroscopy and scanning tunneling microscopy. Electron-momentum spectroscopy [1] is an e, $2e$ scattering technique that can determine the radially averaged density of the outermost valence electrons. Scanning tunneling microscopy [2] gives the electron density, distorted by surface states. We show that high-harmonic emission from molecules [3–9] allows the three-dimensional shape of the highest electronic orbital to be measured, including the relative phase of the components of the wavefunction.

Molecular alignment is achieved via the rotational wavepacket technique: first, an intense but nonionizing laser pulse (60 fs, 10^{13} W/cm^2, "pump") is focused into a supersonic N_2 gas jet. This laser field gives a kick to the molecules towards the laser polarization direction to create rotational wavepackets. Another time-delayed intense laser pulse (30 fs, 3×10^{14} W/cm^2, "probe") is then focused into the gas jet to produce harmonics. Both pulses are linearly polarized in the same direction.

Figure 1 shows the intensities of 19th, 21st, and 29th harmonics as a function of the pump–probe delay. The variation of harmonic intensities agrees well with the degree of molecular alignment $\langle \cos^2\theta \rangle$ (top panel) that was measured in a separate experiment [10]. All orders of harmonics show similar revivals. This result indicates that harmonics are enhanced when molecules are aligned parallel to the field and suppressed when they are perpendicular. The best alignment along the polarization of the pump pulse is achieved at the half revival at a delay of 4.1 ps. We use this revival to create an ensemble of aligned molecules. By rotating the polarization vector of the pump pulse, we are able to rotate

this ensemble relative to the probe pulse's polarization vector.

Figure 2 shows the intensity of harmonics generated from nitrogen molecules aligned at five different angles relative to the polarization axis of the pulse that generates the harmonics.
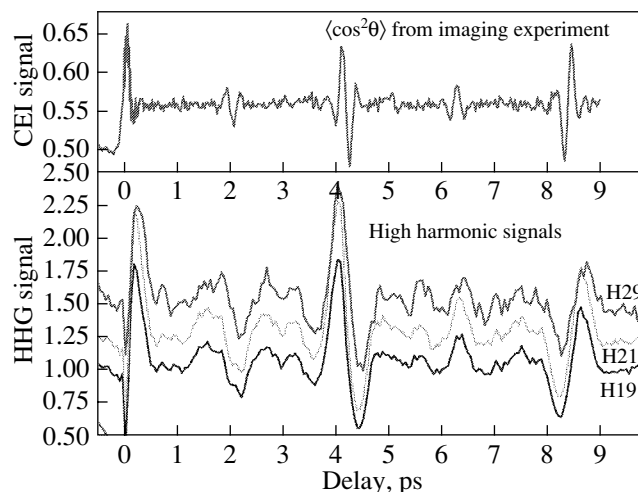
Fig. 1. The lower panel shows the intensity of harmonics 19, 21, and 29 recorded at different pump–probe time delays. The pump pulse at time zero initiates a rotational wavepacket in gas-phase nitrogen. At different times, notably at 4.1 ps, a rotational revival occurs, resulting in a macroscopic alignment of the molecular axis in space. The top panel shows the degree of alignment as quantified by the $\langle \cos^2\theta \rangle$ measurement as recorded in a different experiment. The agreement between the two shows that the harmonic emission is strongest when the molecular axis is parallel to the laser polarization.

Harmonic intensity
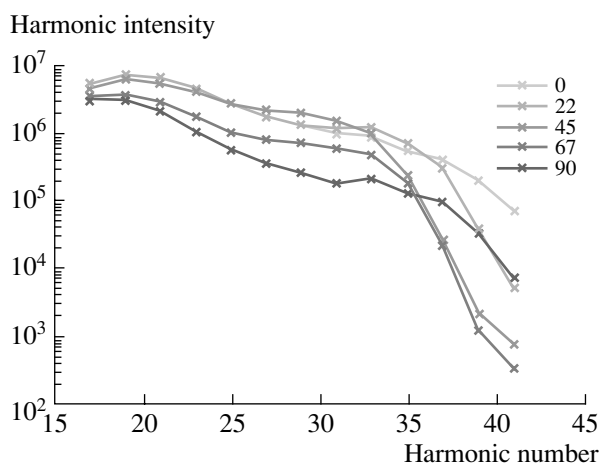
Fig. 2. The high-harmonic spectra were recorded from nitrogen aligned at five different angles relative to the polarization vector of the probe laser. The angles are shown in degrees. There is an order-of-magnitude dependence on the intensity versus angle. These intensities were recorded at a pump–probe time delay of 4.1 ps, corresponding to a revival of the rotational wavepacket.
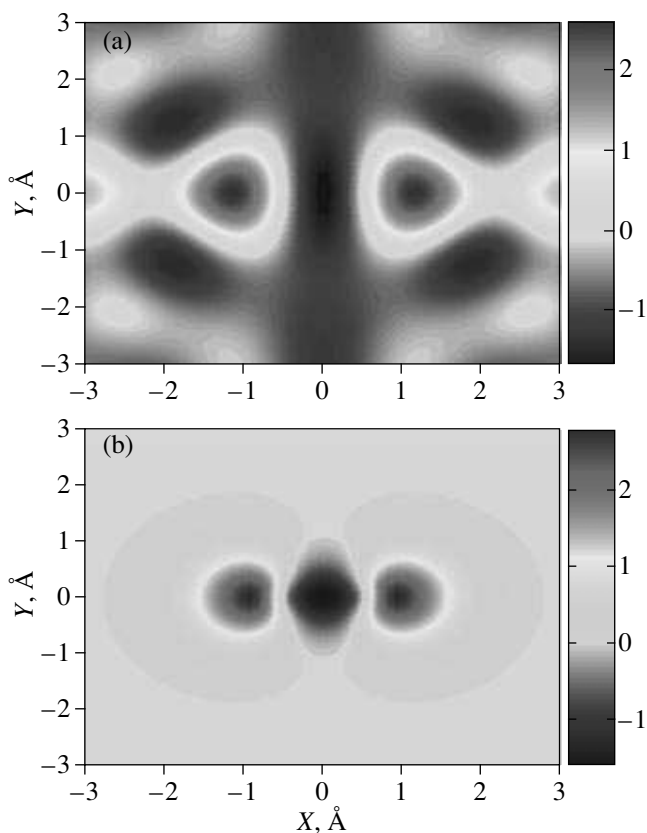
Fig. 3. (a) Shows the reconstruction of the molecular orbital wavefunction of nitrogen. This reconstruction uses a computed tomography algorithm using the data from Fig. 2, as well as a calibration spectrum from argon, whose orbital shape is known. Note that both positive and negative values are present, so this is an actual wavefunction, not the square of the wavefunction. (b) Shows the $N_2 \sigma_g$ orbital shape from an *ab initio* calculation.

Under our experimental conditions, the alignment dependence of tunnel ionization is small (angular variation ~25%) and is approximately canceled by the spatial spread of the electron wavepacket in the continuum. We therefore conclude that the alignment dependence of harmonic intensities is dominated by the recombination process.

When the wavepacket ψ_c recollides with N_2, its lateral spread reaches ~9 Å by quantum diffusion. This size is considerably larger than the size of molecules. The electron wavepacket seen by the molecule can thus be approximated by a chirped plane wave; i.e., $\psi_c = \sum_p A(p)\exp[ipx - iKt]$, where p is the momentum of the electron and $K(= p^2/2)$ is the kinetic energy. The induced dipole is then given by $d(\omega = K) \sim A(p)\langle\psi_g|r|\exp(ipx)\rangle$. This expression is the spatial Fourier transform of $r\Psi_g$ projected onto the direction perpendicular to the laser polarization. Once we know the harmonic spectrum $S(\omega) \sim \omega^4|d(\omega)|^2$, including the spectral phase and polarization, we can deduce the projected wavefunction by inverse Fourier transforming the harmonic spectrum. This is equivalent to measuring the projected images of the wavefunction Ψ_g in different directions. We can therefore reconstruct the image of the bound-state wavefunction by applying the algorithm of computed tomography [11].

We lack knowledge of the complex amplitude $A(p)$ in the plane wave expansion of the continuum wavepacket. To determine $A(p)$, we record the harmonic spectrum of an atom, namely, argon, whose orbital is known. At present we do not measure the phase of each harmonic, although this is possible and has been demonstrated [12]. Figure 3 shows the reconstructed molecular orbital of N_2 compared with the *ab initio* calculation for the HOMO of N_2 (σ_g).

Reconstruction of a single molecular orbital by high-harmonic generation is surprisingly selective to a single orbital. This is due to several properties of the process that work together. (1) Tunnel ionization is selective to the highest occupied orbital due to the nonlinear dependence on ionization potential. (2) The continuum wavepacket is coherent with the orbital wavefunction from which it came (it is the same wavefunction). (3) All electrons in the molecule will radiate in the influence of the returning wavefunction, but only the HOMO will do so coherently. (4) The phase-matching characteristics of HHG that lead to a well-collimated *xuv* beam require that all the molecular emitters be in phase. The emission from all electrons except the HOMO will be randomly phased and will not add coherently.
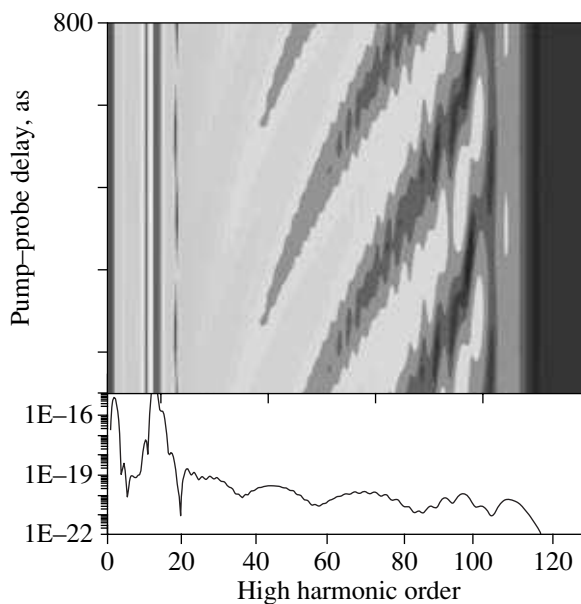
We propose that we can also observe electron wavepacket motion within an atom or molecule using high-harmonic spectra. We argued above that only the highest energy state is seen because only the state that is ionized is coherent with the continuum wavefunction. If we create a coherent superposition of two or more
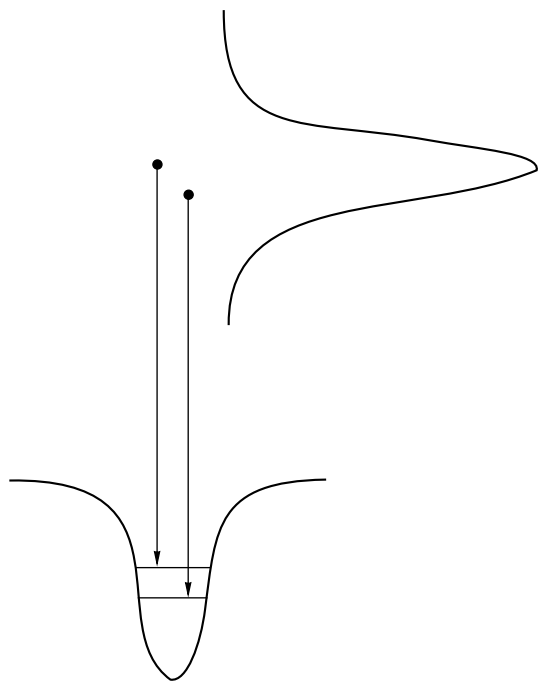
Fig. 4. A schematic diagram shows the bound-state potential at the bottom, with two populated energy levels. The upper curve represents the kinetic-energy distribution of the recolliding continuum electron wavepacket. Even though the continuum wavepacket originates only from the upper bound state, it is coherent with both bound states. The recombination radiation will then show interferences that come from different continuum electron energies that occur at different times in the chirped wavepacket. This will manifest itself as interferences in the high-harmonic spectra.

Fig. 5. A time-dependent Schrödinger equation simulation of an atom with two equally populated bound states shows the interference pattern that reflects the beat frequency between the bound states. The optical field had a wavelength of 1.6 μm and a duration of 8 fs, with mainly a single high-harmonic pulse generated. The energy spacing of the two levels is 9.5 eV, leading to an bound-state electron wavepacket with a period of 435 as. The square of the acceleration of the dipole is plotted as the intensity versus harmonic order. Different pump–probe time delays are shown. The minima in each spectrum come from different electron kinetic energies that lead to the same *xuv* frequency. This simulation shows that it is possible to observe attosecond bound-state electron motion.

electronic states—an electronic wavepacket—then the HHG spectrum will contain information about all the states that compose the wavepacket. Figure 4 shows that interference can occur between two different kinetic-energy portions of the recolliding wavepacket that give the same *xuv* emission frequency. If the period of the wavepacket is shorter than the duration of the chirped returning electron wavepacket, and a few-cycle probe pulse is used, then the motion will be seen as a series of minima in the HHG spectrum. By changing the pump–probe delay, these minima will move in frequency.

To demonstrate how the bound-state wavepacket motion appears in harmonic spectra, we use the one-dimension tune-dependent Schrödinger equation to simulate an electron in a diatomic potential in the presence of an intense laser field. The field is chosen at a wavelength of 1.6 μm and a duration of 8 fs to induce a single recollision. To form a fast-moving bound-state wavepacket, two electronic states with energy difference ΔE = 9.5 eV are equally populated before the arrival of the laser pulse. This energy difference corresponds to wavepacket motion with a period of 435 as. By varying the initial phase of the two states, we per-

form a numerical pump–probe measurement of the wavepacket motion.

Figure 5 shows the calculated harmonic spectrum versus the initial phase of the two states. The structure in the harmonic spectrum synchronizes with the bound-state wavepacket motion. Both the modulation in the single time delay spectrum and the movement of the modulation in the pump–probe spectrum measure wavepacket dynamics.

ACKNOWLEDGMENTS

REFERENCES

1. C. E. Brion, G. Cooper, Y. Zheng, *et al.*, "Imaging of Orbital Electron Densities by Electron Momentum Spectroscopy—a Chemical Interpretation of the Binary (*e*, 2*e*) Reaction," Chem. Phys. **270**, 13 (2001).

2. G. Binning, H. Rohrer, Ch. Gerber, and E. Weibel, "Surface Studies by Scanning Tunneling Microscopy," Phys. Rev. Lett. **49**, 57 (1982).

3. H. Sakai and K. Miyazaki, "High-Order Harmonic Generation in Nitrogen Molecules with Subpicosecond Visible Dye-laser Pulses," Appl. Phys. B **61**, 493 (1995).

4. Y. Liang, A. Augst, S. L. Chin, *et al.*, "High Harmonic Generation in Atomic and Diatomic Molecular Gases Using Intense Picosecond Laser Pulses—A Comparison," J. Phys. B **27**, 5119 (1994).

5. R. Velotta, N. Hay, M. B. Manson, *et al.*, "High-Order Harmonic Generation in Aligned Molecules," Phys. Rev. Lett. **87**, 183901 (2001).

6. R. de Nalda, E. Heesel, M. Lein, *et al.*, "Role of Orbital Symmetry in High-Order Harmonic Generation from Aligned Molecules," Phys. Rev. A **69**, 031804(R) (2004).

7. N. Hay, M. Lein, R. Velotta, *et al.*, "Investigations of Electron Wave-Packet Dynamics and High-Order Harmonic Generation in Laser-aligned Molecules," J. Mod. Opt. **50**, 561 (2003).

8. N. Hay, R. Velotta, M. Lein, *et al.*, "High-Order Harmonic Generation in Laser-aligned Molecules," Phys. Rev. A **65**, 053805 (2002).

9. M. Lein, P. P. Corso, J. P. Marangos, and P. L. Knight, "Orientation Dependence of High-Order Harmonic Generation in Molecules," Phys. Rev. A **67**, 023819 (2003).

10. P. W. Dooley, I. V. Litvinyuk, K. F. Lee, *et al.*, "Direct Imaging of Rotational Wave-Packet Dynamics of Diatomic Molecules," Phys. Rev. A **68**, 023406 (2003).

11. C. Kak and M. Slaney, *Principles of Computerized Tomographic Imaging* (Society for Industrial and Applied Mathematics, New York, 2001).

12. Y. Mairesse, A. de Bohan, L. J. Frasinski, *et al.*, "Attosecond Synchronization of High-Harmonic Soft X-rays," Science **302**, 1540 (2003).